Damage Percolation Modeling of Void Nucleation in Aluminum Alloy Sheet

C.J. Butcher, Z.T. Chen
University of New Brunswick, Fredericton, Canada

Abstract

Damage-induced ductile fracture is a strongly heterogeneous process where micro-voids nucleate, grow and coalesce within particle clusters. To capture the localized nature of ductile fracture, a damage percolation model has been developed to predict damage development in the actual particle distribution obtained from tessellated particle fields. Percolation modeling allows for the characterization of void nucleation and coalescence under various loading conditions within a heterogeneous particle distribution. Particularly, void nucleation can be characterized under different stress states for individual particles. The objective of the present work is to apply the percolation model to a damage-sensitive aluminum alloy, AA5182, to develop a nucleation criterion as a function of stress state and particle morphology. The nucleation model is calibrated by subjecting three particle fields to different levels of uniaxial and biaxial stretching in order to achieve fracture predictions in agreement with an experimental forming limit curve.

Introduction

The automotive industry has recently turned to using advanced high strength steel and aluminum alloys to produce high quality components with reduced weight and improved fuel economy. However, these alloys experience poor formability due to the presence of second-phase particles which crack or debond to form microvoids (damage). These microvoids grow and link-up to form cracks, resulting in sudden fracture during forming. Due to the complex nature of damage-induced ductile fracture, traditionally damage-based constitutive models have been developed which homogenize void damage throughout the material [1-3]. However, ductile fracture is a highly localized phenomenon with void nucleation, growth and coalescence originating in heterogeneous particle clusters [4].

The influence of heterogeneous particle distributions on ductile fracture can be captured using the so-called damage percolation modeling [4-6]. In the damage percolation model, digital imaging techniques are used to obtain the actual particle distribution in a material. Using this information, micromechanical models are applied to characterize void and crack formation leading to failure at an individual particle scale. The percolation model captures the localized nature of ductile fracture as nucleation, growth and coalescence originate within particle clusters. A particle field loaded in equal-biaxial tension is presented in Figure 1 with the second phase particles appearing as shaded black and the grey ellipses representing the approximate crack size. The damage percolation model represents the next

generation in modeling ductile fracture by relating changes in the local microstructure to the overall material behaviour.

The current damage percolation model of Worswick et al. [4-6] cannot make deterministic predictions of fracture since the void nucleation and coalescence criteria are based solely upon geometric considerations and thus neglect the stress state. Void growth is strain-controlled and is well represented in the percolation model. Recent void coalescence models have been proposed where coalescence is a function of the stress state and void geometry which are well suited for implementation into the percolation model [3, 7]. The fracture predictions of the percolation model are extremely sensitive to the void nucleation rule [4]. Nucleation is often modeled using bulk criteria which are unsuitable for the purpose of percolation modeling since nucleation occurs at the individual particle scale. The objective of the present work is to develop and calibrate a nucleation criterion for the damage percolation model where nucleation is a function of the stress state and particle morphology. The nucleation model is calibrated using an experimental forming limit curve for aluminum AA5182 sheet.

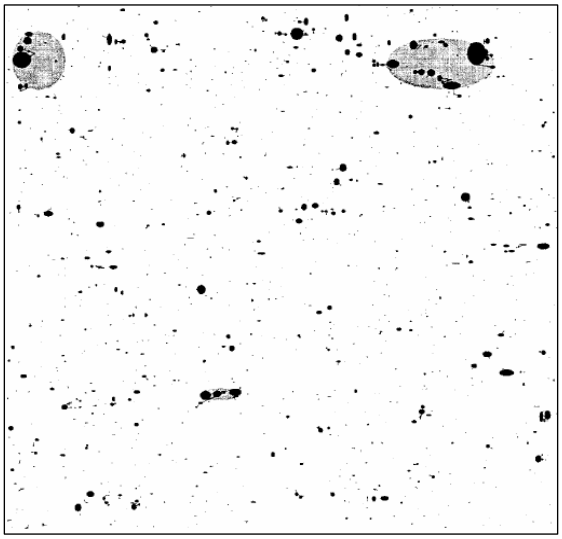

Figure 1. Predicted damage in an AA5182 particle field. Rolling direction is vertical [4].

2. Derivation of the nucleation criterion for percolation modeling

Void nucleation primarily occurs at second phase particles via particle cracking or separation of the particle-matrix interface (debonding). A realistic nucleation criterion should account for many factors such as the nucleation mechanism (cracking or debonding), particle morphology (size, shape, clustering and volume fraction) and stress state. Additional factors which can influence void nucleation are the strain rate, temperature and level of pre-strain in the material [8]. In the present work, a phenomenological nucleation model is developed where the nucleation strain is assumed to be a function of the particle morphology and stress state of the form

$$\varepsilon_{\mathrm{N}} = \varepsilon_{\mathrm{N_o}}\, g(d) h(f_{\mathrm{n}}) s(T, \mu_L) \tag{1}$$

where $\varepsilon_{\mathrm{N_o}}$ is the nucleation strain in pure shear which is scaled by weighting functions related to the particle diameter, d, area fraction of second phase particles,

f_n, and stress state defined by the stress triaxiality, T, and Lode parameter, μ_L. The influence of particle clustering and aspect ratio on void nucleation is not accounted for in the present work. No assumptions are made regarding the nucleation mechanism since the mean particle aspect ratio in AA5182 sheet is essentially spherical and thus nucleation is a competition between particle cracking and interface separation [9].

2.1. Particle size

In general, the strain required to nucleate a void is inversely related to particle size with larger particles nucleating at lower strains [10-12]. The particle size-related parameter of Horstemeyer et al. [13] is adopted and is related to the nucleation strain as

$$g(d) = \frac{1}{\sqrt{d}} = \left(\frac{4}{\pi} A_p \right)^{-0.25} \tag{2}$$

where d is the particle diameter and A_p is the particle area.

2.2. Particle area fraction

While it is reasonable to assume that the more second phase particles, the greater the chance for nucleation, the opposite has been observed experimentally [14, 15]. Here, we assume that the nucleation strain increase with the area fraction of second phase particles as

$$h(f_n) = f_n^{1/3} \tag{3}$$

where the exponent of one-third is selected based upon the work of Gangalee and Gurland [14] who observed that the ratio of $\sqrt{d} / f_n^{1/3}$ was useful for a range of particle sizes and area fractions in aluminum-silicon alloys. The product of the size and area fraction functions, $g(d)h(f_n)$, results in the inverse of this ratio as we assume the nucleation strain decreases with particle size and increases with the second phase particle content. The nucleation model of Horstemeyer et al. [13] also exhibits a dependence upon $\sqrt{d} / f_n^{1/3}$ which acts as a scaling factor for the nucleation rate.

2.3. Stress state

The nucleation strain has been shown to decrease with increasing stress triaxiality [12]; however, the stress triaxiality alone is insufficient to uniquely characterize the stress state since it is a measure of only two of the three stress invariants: the

equivalent and mean stress. Consequently, for a given triaxiality, the severity of shear loading is unknown. The shear or deviatoric stress state can be characterized by incorporating a dependence upon the third stress invariant using the Lode parameter, μ_{L}. The stress state can be uniquely described using the stress triaxiality and Lode parameter

$$T = \frac{\sigma_1 + \sigma_2 + \sigma_3}{3\sigma_{\mathrm{eq}}} = \frac{\sigma_{\mathrm{hyd}}}{\sigma_{\mathrm{eq}}} \qquad \mu_{\mathrm{L}} = \frac{2\sigma_2 - \sigma_1 - \sigma_3}{\sigma_1 - \sigma_3} = \frac{3(\sigma_2 - \sigma_{\mathrm{hyd}})}{\sigma_1 - \sigma_3} \tag{4, 5}$$

where σ_{hyd} is the hydrostatic stress, σ_{eq} is the equivalent stress and σ_1, σ_2, σ_3 are the principal stresses in descending order. The stress triaxialities corresponding to uniaxial tension, plane strain and equal-biaxial tension are: $1/3$, $1/\sqrt{3}$ and $2/3$, respectively. Lode parameters of -1, 0 and 1 correspond to uniaxial tension, generalized shear and equal-biaxial tension, respectively, with all other values representing a state of combined tension and shear.

While the influence of shearing on void nucleation has often been neglected, the nucleation model of Horstmeyer et al. [13] included a dependence upon the third stress invariant which predicted a higher nucleation rate in combined tension and torsion compared to pure tension. Furthermore, Dighe et al. [11] experimentally observed a higher degree of particle cracking in torsion than in tension for an Al-Si alloy. A very recent study by Maire et al. [16] observed that the nucleation strain in a dual phase steel could be well described by the stress triaxiality in uniaxial tension. For a general material, the nucleation rule used by Maire et al. [16] can be written as

$$\varepsilon_{\mathrm{N}} = \varepsilon_{\mathrm{No}} \exp\left(-kT\right) \tag{6}$$

where $\varepsilon_{\mathrm{No}}$ is the nucleation strain corresponding to pure shear ($T = 0$) and k is the triaxiality scale factor identified through calibration with experiment data. However, since many different shear stress states can be obtained for the same triaxiality, the scale factor would almost certainly change if it was identified in a state of combined tension and shear rather than uniaxial tension. Therefore, we propose a phenomenological relationship for the triaxiality scale factor as a function of the Lode parameter

$$k\left(\mu_L\right) = \left(2 - \beta\left|\mu_L\right|\right) \tag{7}$$

where β is an adjustable parameter. The value of 2 in Eq. (7) was arbitrarily selected so that $k = 1$ in tension if $\beta = 1$. For simplicity, we make no distinction between the Lode parameter in uniaxial and biaxial tension [17]. The stress state weighting function, $s(T, \mu_L)$ in Eq. (1) is extracted from Eq. (6) and (7) as

$$s(T,\mu_L) = \exp\left[-T\left(2-\beta\left|\mu_L\right|\right)\right] \tag{8}$$

2.1.4 Nucleation model

Since the nucleation model will be applied to different particle fields the particle morphology should be measured relative to the average morphology and the nucleation model is expressed as

$$\varepsilon_N = \varepsilon_{No}\left(\frac{f_n}{f_{n\text{-}avg}}\right)^{\frac{1}{3}}\left(\frac{A}{A_{avg}}\right)^{\frac{-1}{4}} \exp\left[-T\left(2-\beta\left|\mu_L\right|\right)\right] \tag{9}$$

where A_{avg} and $f_{n\text{-}avg}$ are the average particle area and area fraction for all particle fields. In the present work, the nucleation parameters ε_{No} and β are identified through calibration of the percolation model with an experimental forming limit curve. The nucleation values could also have been determined using torsion and tensile test data. The general trend for the variation of the nucleation strain with particle size and stress state is presented in Figure 2.

The proposed nucleation model reflects the contribution of shear loading as the nucleation strain is lower in plane strain than equal-biaxial tension even though the triaxiality is smaller. A similar trend is observed in forming limit diagrams where the limit strain decreases from uniaxial tension to plane strain (triaxiality and shear loading increasing). The forming limit then increases as an equal-biaxial condition is approached (triaxiality increasing, shear loading decreasing). A tensile and shear stress state will also promote void coalescence.

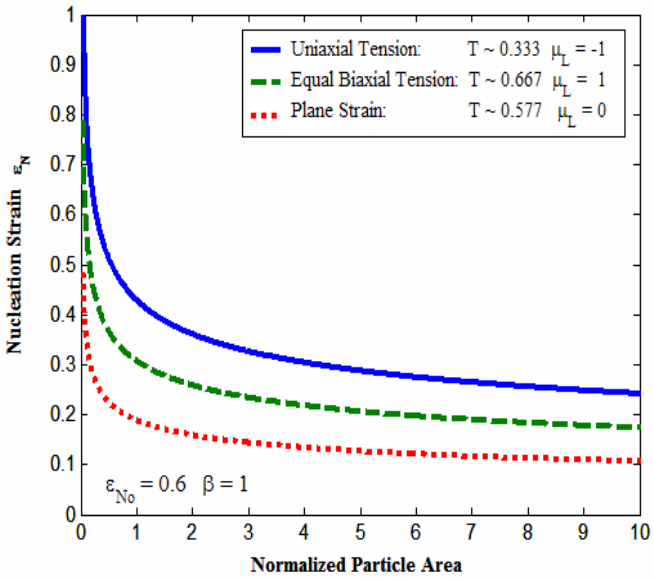

Figure 2. Variation of the nucleation strain with particle size and stress state.

3. Percolation modeling of ductile fracture

Worswick et al. [4] developed the so-called damage percolation model to account for the heterogeneous void and particle distributions in aluminum-magnesium alloys. Chen et al. [5, 6] linked the percolation model with a commercial finite-

element code to investigate localized damage initiation in the stretch flange forming of aluminum sheet. The development of the percolation model is quite extensive and is discussed in detail in [4, 5]. For brevity, only a summarized discussion is provided.

A large-scale high-resolution digital image of a second phase particle field of AA5182 sheet was acquired from the planar metallographic view [4]. The particle feature data is extracted using a matrix erosion tessellation algorithm to obtain the particle centroid coordinates, principal axes, nearest neighbour list and cluster lists (particles comprising each cluster). The particles are assumed to be elliptical and aligned in either the rolling or transverse direction. No distinction is made between the Fe and Mn-based intermetallic particles in the alloy. Void nucleation, growth and coalescence criterion are treated using different criteria.

3.1. Stress integration

The global particle field (including particles and matrix) is assumed to obey the Gurson-Tvergaard [1,2] yield criterion to account for material softening and is written as

$$\Phi = \frac{\sigma_{\text{eq}}{}^2}{\bar{\sigma}^2} + 2fq_1 \cosh\left(q_2 \frac{3}{2}\frac{\sigma_{\text{hyd}}}{\bar{\sigma}}\right) - \left(q_1 f\right)^2 - 1 = 0 \tag{10}$$

where f is the area fraction of voids in the particle field, $\bar{\sigma}$ is the material flow stress and q_1, q_2 are Tvergaard's [2] calibration parameters with $q_1 = 1.25$, $q_2 = 0.95$ for AA5182 sheet [6]. The flow stress relation for AA5182 sheet is $\bar{\sigma} = 139 + 334.5\exp\left(-4.062\varepsilon^{\text{p}}\right)$ (MPa) [18] where ε^{p} is the effective plastic strain.

3.2. Void nucleation

The void nucleation criterion derived in Eq. (9) has been incorporated into the percolation model and applied to each particle for each time-step in the stress integration routine. The dimensions of the nucleated void are assumed to be equal to the particle dimensions.

3.3. Void growth

Void growth is modeled using the results of unit cell calculations by Thomson et al. [19] and the void growth rate is a function of the strain state and void aspect ratio. The influence of void clustering on the growth rate is currently not considered. The growth rates were obtained from the unit cell calculations for an isolated void.

3.4. Void coalescence

The previous coalescence rule used in the percolation model in [4-6] was a modified Brown and Embury [20] criterion independent of the stress state. Thomason [7] has derived a void coalescence model based upon necking failure of the intervoid ligament where coalescence occurs as a function of the stress state and void geometry. Coalescence occurs in Thomason's [7] so-called plastic limit-load when

$$\frac{\sigma_1}{\bar{\sigma}} \geq \frac{2}{\sqrt{3}}\left(\sqrt{1+\frac{1}{4\tan^2\psi}}+\frac{\chi^{-1}-1}{4\lambda}\right)(1-\chi) \tag{11}$$

where ψ is the angle of the maximum principal stress relative to the material ligament; λ is the void aspect ratio (R_y / R_x), and χ is the void spacing ratio defined as the ratio of the lateral void radius to half of the lateral void spacing. However, the void distribution in a real material is not periodic as idealized in the plastic limit-load criterion. Therefore, the geometrical parameters in Eq. (11) are determined using a local coordinate system defined using the ligament orientation angle, θ, as shown in Figure 3. The void aspect and spacing ratios are defined as

$$\lambda = \frac{R_{y1}' + R_{y2}'}{R_{x1}' + R_{x2}'} \tag{12}$$

$$\chi = \frac{R_{x1}' + R_{x2}'}{c} \tag{13}$$

where c is the center-to-center distance between voids and Eq. (11) is evaluated at each time-step for all neighbouring pairs of nucleated voids.

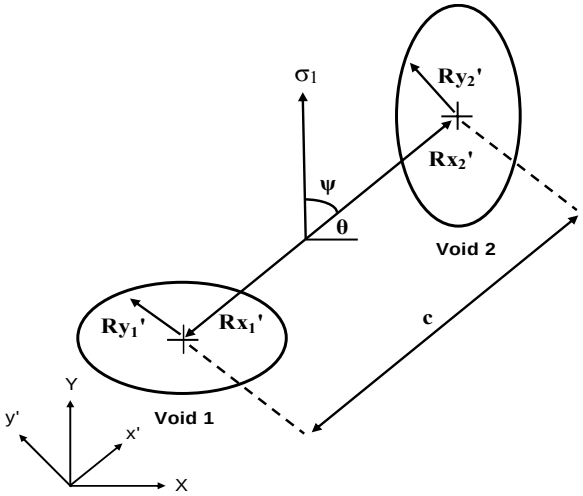

Figure 3. Schematic of interaction geometry.

It is important to mention that coalescence can also occur due to ligament shearing or a combination of necking and shearing but these mechanisms are not considered in the present coalescence model.

3.5. Post-coalescence treatment

Once two voids have coalesced they are treated as a larger elliptical void or 'crack' to model the amplified interaction effect between small and large voids. The size of the coalesced void is determined such that both voids are contained within a

bounding rectangle. This newly formed large void can thus coalesce with neighbouring voids and propagate throughout the material leading to profuse coalescence and failure.

4. Material

Three tessellated particle fields are considered with each field corresponding to 2000 x 2000 pixels or 0.75 mm x 0.75 mm. The material is assumed to be initially damage free. The particle aspect ratio and spacing ratio are calculated using Eq. (12) and (13), respectively. The second phase particles exhibit significant clustering as evidenced by the large particle spacing ratio. Therefore, coalescence can be expected to occur shortly after nucleation. The particle field data is summarized in Table 1.

Table 1. Particle field information for AA5182 sheet.

Particle Field	Initial Particle Area Fraction f_n	Particle Area A (μm^2)	Particle Aspect Ratio λ_p	Particle Spacing Ratio χ_p
P1	0.0177	7.876	1.20	0.618
P2	0.0142	5.416	1.25	0.562
P3	0.0079	4.208	1.24	0.531
Average	0.0133	5.833	1.23	0.570

5. Calibration of the nucleation model

The nucleation parameters in Eq. (9) are identified parametrically by comparing the fracture predictions of the percolation model for each particle field with the experimental forming limit curve data of Brunet et al. [18] for 1 mm thick AA5182 sheet. Each particle field is subjected to a range of proportional straining (ratio of the minor to major strain) from -0.5 (uniaxial tension) to one (equal biaxial stretching) with the limit strain detected at the onset of profuse coalescence. For each strain ratio, the particle field is loaded in both the rolling and transverse directions. The particle field is assumed to deform homogeneously and remain rectangular throughout the deformation process.

6. Results and discussion

The forming limit predictions for each particle field in the rolling and transverse directions are compared with the experimental data in Figure 4. The forming limit curve obtained using the percolation model gives very good agreement with the experiment data for nucleation parameters of $\varepsilon_{No} = 0.50$ and $\beta = 1.80$. The forming

limit predictions are similar for particle fields P1 and P3 with P2 predicting the highest limit strains. Overall, the scatter in the predictions of the percolation model is reasonable considering that the particle fields are very different. As in a real material, a particle field may result in lower fracture predictions if it contains an excessive degree of particle clustering.

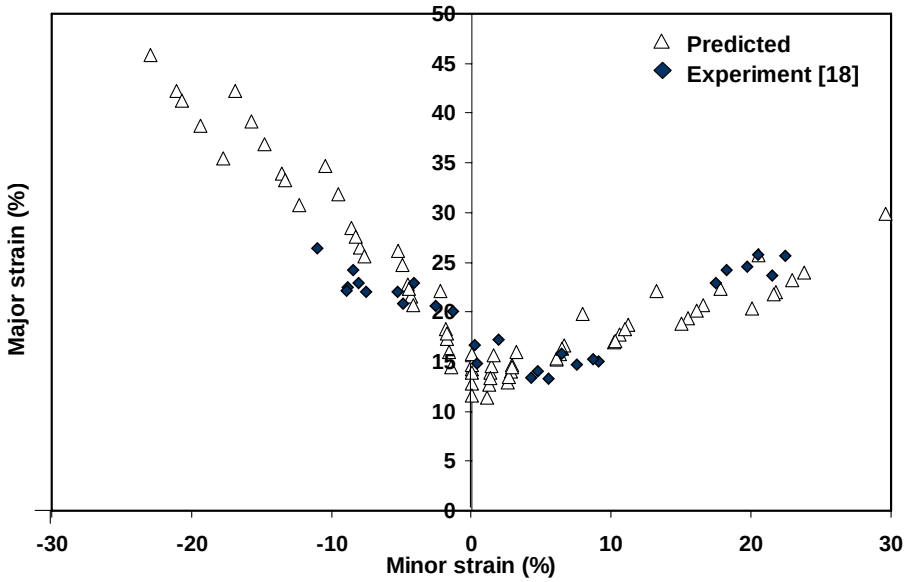

Figure 4. Comparison of the predicted forming limit data with the experiment results of Brunet et al. [18].

7. Conclusions

A phenomenological void nucleation criterion has been developed for implementation into a damage percolation model where nucleation occurs at the individual particle scale as a function of the particle morphology and stress state. The stress state is characterized by incorporating a dependence upon the stress triaxiality and severity of shear loading using the Lode parameter. The nucleation rule has been applied to the percolation modeling of AA5182 sheet and achieved excellent agreement with an experimental forming limit curve with ε_{No} = 0.50 and $\beta = 1.80$. The current research provides a valuable tool for relating damage initiation within particle clusters at the micro-scale with the macroscopic behaviour of the bulk material.

References

[1] A.L. Gurson, Continuum theory of ductile rupture by void nucleation and growth – Part I. Yield criteria and flow rules for porous ductile media, J. Eng. Mater. Tech. 99 (1977) 2-15

[2] V. Tvergaard, Influence of voids on shear band instabilities under plane strain

conditions, Int. J. Frac. 17 (1981) 389-407.
[3] A.A. Benzerga, Micromechanics of coalescence in ductile fracture, J. Mech. Phys. Solids 50 (2002) 1331-1362.
[4] M.J. Worswick, Z.T. Chen, A.K. Pilkey, D. Lloyd, S. Court, Damage characterization and damage percolation modeling in aluminum alloy sheet, Acta Mater. 49 (2001) 2791-2803.
[5] Z.T. Chen, M.J. Worswick, N. Cinotti, A.K. Pilkey, D. Lloyd, A linked FEM-damage percolation model of aluminum alloy sheet forming, Int. J. Plasticity 19 (2003) 2099-2120.
[6] Z.T. Chen, M.J. Worswick, A.K. Pilkey, D.J. Lloyd, Damage percolation during stretch flange forming of aluminum alloy sheet, J. Mech. Phys. Solids 53 (2005) 2692-2717.
[7] P.F. Thomason, P.F, Ductile fracture of metals, Pergamon Press, Oxford, 1990
[8] M.F. Horstemeyer, S. Ramaswamy, M. Negrete, Using a micromechanical finite element parametric study to motivate a phenomenological macroscale model for void/crack nucleation in aluminum with a hard second phase, Mech. Mater. 35 (2003) 675-687.
[9] D. Lassance, F. Scheyvaerts, T. Pardoen, Growth and coalescence of penny-shaped voids in metallic alloys, Eng. Fract. Mech. 73 (2006) 1009-1034.
[10] J.D. Embury, Plastic flow in dispersion hardened materials, Metall. Trans. A 16 (1985) 2191-2200.
[11] M.D. Dighe, A.M. Gokhale, M.F. Horstemeyer, Second phase cracking and debonding observations in the fatigue damage evolution of a cast Al-Si-Mg alloy, Metall. Mater. Trans A 38 (2002) 1-8.
[12] M. N. Shabrov, A. Needleman, An analysis of inclusion morphology effects on void nucleation, Model. Sim. Mater. Sci. Eng. 10 (2002) 163-183.
[13] M.F. Horstemeyer, A.M. Gokhale, A void-crack nucleation model for ductile metals, Int. J. Solids. Struct. 36 (1999) 5029-5055.
[14] A. Gangalee, J. Gurland, On the fracture of silicon particles in aluminum-silicon alloys, Trans. Metall. Soc. of AIME 239 (1967) 269-272.
[15] M. Mazinani, W.J. Poole, Effect of plasticity on the deformation behavior of a low-carbon dual phase steel, Metall. Mater. Trans. A. 38 (2007) 328-339.
[16] E. Maire, O. Bouaziz, M. Di Michiel, C. Verdu, Initiation and growth of damage in a dual-phase steel observed by X-ray microtomography, Acta Mater. 56 (2008), 4954-4964.
[17] L. Xue, Constitutive modeling of void shearing effect in ductile fracture of porous materials, Eng. Frac. Mech. 75 (2007) 3343-3366.
[18] M. Brunet, Morestin, F., H. Walter-Leberre, Failure analysis of anisotropic sheet-metals using a non-local plastic damage model, J. Mater. Proc. Tech. 170 (2005) 457-470.
[19] C.I.A. Thomson, M.J. Worswick, A.K. Pilkey, D.J. Lloyd, G. Burger, Modeling void nucleation and growth within periodic clusters of particles, J. Mech. Phys. Solids 47 (1999) 1-26.
[20] L.M. Brown, Embury, J.D., The initiation and growth of voids at second phase particles, Proc. 3rd Int. Conf. Strength of Metals and Alloys, Institute of Metals, London, 1973, pp. 164-169.